Phase dynamics in SQUID's: Anomalous diffusion and irregular energy dependence of diffusion coefficients

Ken-ichi Tanimoto,* Takeo Kato, and Katsuhiro Nakamura
Department of Applied Physics, Osaka City University, Sumiyoshi-ku, Osaka 558-8585, Japan
(Received 16 March 2002; published 24 June 2002)

Deterministic diffusions of superconducting phases in extremely underdamped SQUID's are studied. It is found that, by controlling the total energy, two types of diffusion, i.e., anomalous and normal ones, appear. In the anomalous diffusion, the orbit in the phase space is trapped mainly into the jump-related hierarchy structure so that the mean-square displacement behaves as t^{γ} with $1<\gamma<2$. This enhanced diffusion is analyzed from a viewpoint of the Lévy walk. Even in the normal diffusion, it is revealed that the diffusion coefficient has the amazing irregular energy dependence, which reflects an extreme sensitivity of the phase-space structure to a small change of the energy.

DOI: 10.1103/PhysRevB.66.012507 PACS number(s): 05.45.−a, 74.50.+r, 05.40.Fb, 05.60.Cd

Deterministic diffusion phenomena and their statistical properties have received a wide attention for more than two decades.[1–4] In many deterministic systems, the nature of diffusions shows an anomalous feature, which is characterized by anomalous exponents of time in mean square displacements. This anomalous diffusion (AD) has been studied in dissipative systems including low-dimensional maps,[5,6] overdamped Josephson junctions,[7,8] and two-dimensional flow.[9] AD in Hamiltonian systems has also been studied in, for example, two-dimensional Hamiltonian systems.[10,11] We, however, have as yet little knowledge on AD in experimentally realizable Hamiltonian systems which are free from disorders such as impurities.

Recently, Klages and Dorfman have pointed out that even in deterministic normal diffusions (ND), the diffusion constant may show an irregular fractal structure as a function of a model parameter.[3,12] They have analyzed a chaotic map with one-dimensional piecewise linear chains with a uniform slope, and have shown that the diffusion coefficient has a fractal structure as a function of the slope of a map. The fractal-like structure of diffusion constants in Hamiltonian systems has also been studied in systems where a point particle is subject to constant gravity and is bouncing on a one-dimensional periodically corrugated hard floor.[13] It, however, is also highly desirable to reveal this novel feature in more experimentally accessible systems.

In this paper, we propose an extremely underdamped SQUID as a promising candidate in which both the AD and ND of Hamiltonian systems can be studied. The basic nature of this dynamical system has been studied for a few decades.[14,15] Because of the macroscopic nature of its phase, the SQUID system is more robust to microscopic impurities or/and inhomogeneities than ones proposed previously.[2,13] Moreover, the SQUID system has a great advantage in controlling the total energy E and other model parameters by changing initial conditions and external magnetic field in one

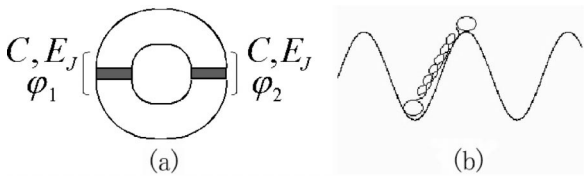

FIG. 1. (a) SQUID with two Josephson junctions. Black and white regions are insulator and superconductor, respectively. The dynamics is described by phase differences φ_1 and φ_2. (b) Equivalent molecule model with a cosine potential.

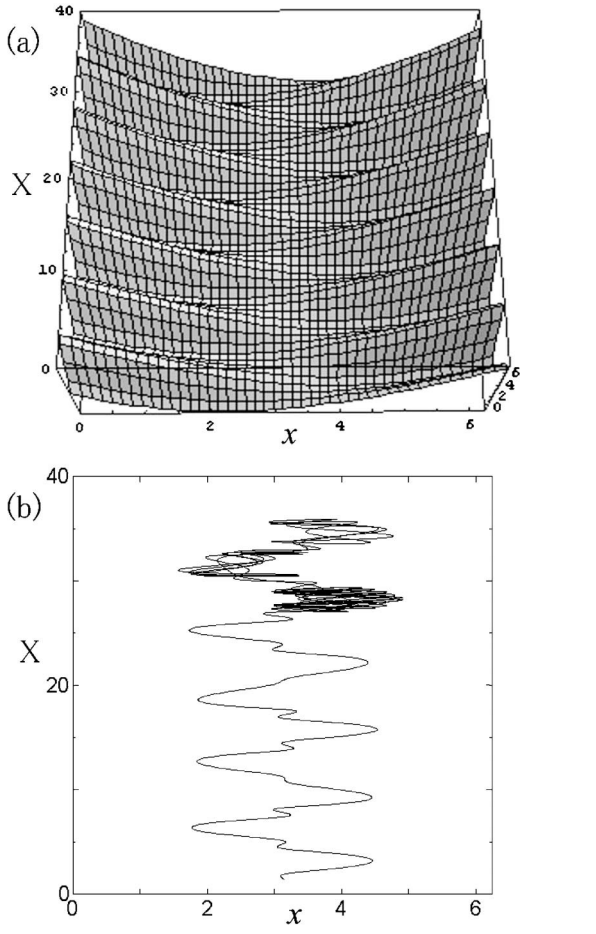

FIG. 2. Phase dynamics in the two-dimensional potential. Horizontal and vertical axes correspond to relative and center-of-mass coordinates, respectively. (a) The shape of two-dimensional potential and (b) an example of a trajectory.

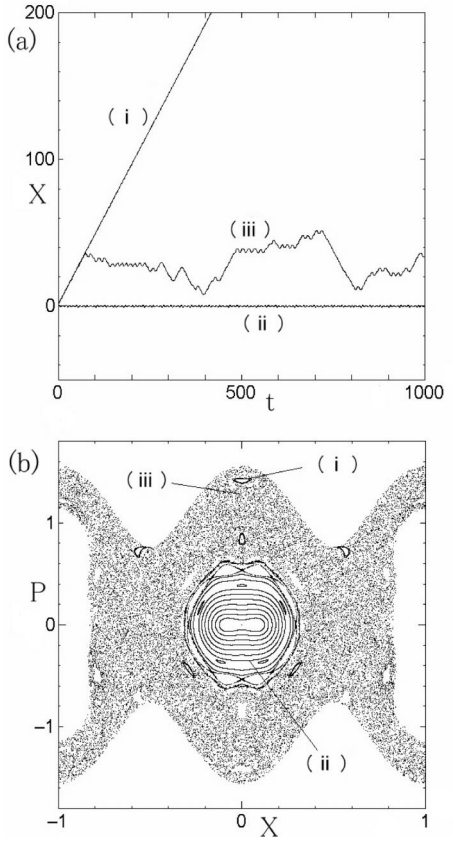

FIG. 3. (a) Time series of the center-of-mass coordinate at $E=0.61$ for three types of orbits: (i) drift orbit, (ii) trapped-periodic orbit, (iii) chaotic orbit. (b) Underlying Poincaré section with $p=0$ and $E=0.61$.

sample.[14,15] Therefore we can see the nature of both AD and ND simply by tuning the energy and model parameter.

Let us introduce a SQUID model consisting of two Josephson junctions shown in Fig. 1(a). The dynamics of this SQUID is described by superconducting phase differences φ_1 and φ_2. The Lagrangian is given as $L=K-U$, where

$$K=\frac{1}{2}C\left(\frac{\Phi_0}{2\pi}\dot{\varphi}_1\right)^2+\frac{1}{2}C\left(\frac{\Phi_0}{2\pi}\dot{\varphi}_2\right)^2, \tag{1}$$

$$U=-E_J\cos\varphi_1-E_J\cos\varphi_2+\frac{1}{2L}\left(\frac{\Phi_0}{2\pi}\right)^2(\varphi_2-\varphi_1-a)^2. \tag{2}$$

The kinetic energy K corresponds to the charging energy, while the potential energy U corresponds to the sum of the Josephson energy and inductance energy. Here, C, E_J, and L are the capacitance, the Josephson energy of each junction, and the inductance of the superconducting loop, respectively. The external flux Φ_e penetrating the loop changes the parameter a in Eq. (2) through $a=2\pi\Phi_e/\Phi_0$, where $\Phi_0=h/2e$ is a unit flux. By defining dimensionless parameters as $V_0=E_J/E_0$ and $\tilde{\mathcal{L}}=\mathcal{L}/E_0$ via $E_0=(\Phi_0/2\pi)^2/L$, and by normalizing the time as $\tilde{t}=\omega t$ via $\omega=\sqrt{LC}$, the Lagrangian is reduced to

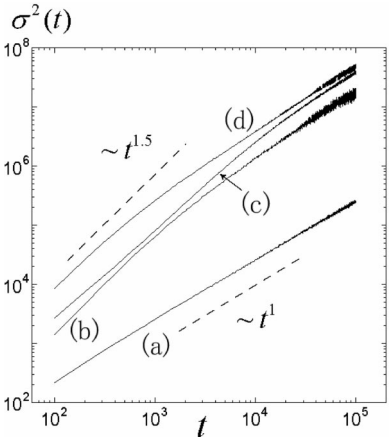

FIG. 4. Mean square displacements (MSD): (a) at $E=0.61$, (b) at $E=1.26$, (c) at $E=3.01$, (d) at $E=6.21$.

$$\tilde{\mathcal{L}}=\tfrac{1}{2}\dot{\tilde{\varphi}}_1^2+\tfrac{1}{2}\dot{\tilde{\varphi}}_2^2+V_0\cos\varphi_1+V_0\cos\varphi_2-\tfrac{1}{2}(\varphi_2-\varphi_1-a)^2. \tag{3}$$

This model turns out to be equivalent to that of two coupled particles in a cosine potential [see Fig. 1(b)]. Below, we neglect quantum effects on the phase dynamics by assuming that the normalized Plank constant $\bar{\hbar}=\hbar\omega/E_0$ is small enough. We also assume the damping effect is so weak that the system behaves as a Hamiltonian system in the relevant time scale.

To simplify the analysis, we employ the center-of-mass and relative coordinates $X=(\varphi_1+\varphi_2)/2$ and $x=\varphi_2-\varphi_1$, respectively. With use of $P=\partial\tilde{\mathcal{L}}/\partial\dot{X}=2\dot{X}, p=\partial\tilde{\mathcal{L}}/\partial\dot{x}=\dot{x}/2$, the resultant Hamiltonian becomes

$$H=\tfrac{1}{4}\dot{P}^2+\dot{p}^2+\tilde{U}(X,x), \tag{4a}$$

$$\tilde{U}(X,x)=-2V_0\cos(X)\cos(x/2)+\tfrac{1}{2}(x-a)^2. \tag{4b}$$

In this system, the total energy E can be controlled by changing the parameter a by the magnetic flux as follows. When the particle is relaxed to the potential minimum at $a=a_1$, and when a is changed to another value a_2 immediately, the particle begins to move in the two-dimensional potential with a constant energy E, until the damping effect appears. Thus, E is controlled by a_1 and a_2 experimentally. Below, we treat the total energy E as a control parameter.

The Hamiltonian (4a) describes a nonintegrable system which exhibits dynamical chaos. We numerically analyze the equations of motion derived from Eq. (4a) by the fourth simplectic integration method with a typical time slice $\Delta t=0.001$–0.01. To see anomalous features of diffusions most easily, a is chosen as π corresponding to one half of the periodicity of the potential. In these circumstances, the potential $\tilde{U}$ has minima at $X=n\pi$, while the saddle points lie on $X=(2n+1)\pi/2$, where n is an integer. Below, we discuss AD by taking V_0 as 1, while ND by taking V_0 as 2. The saddle-point energy measured from the potential minima is given as $E_{\text{saddle}}=0.456$ for $V_0=1$, and as $E_{\text{saddle}}=1.60$ for $V_0=2$, respectively. In both cases, the diffusion occurs only for $E>E_{\text{saddle}}$.

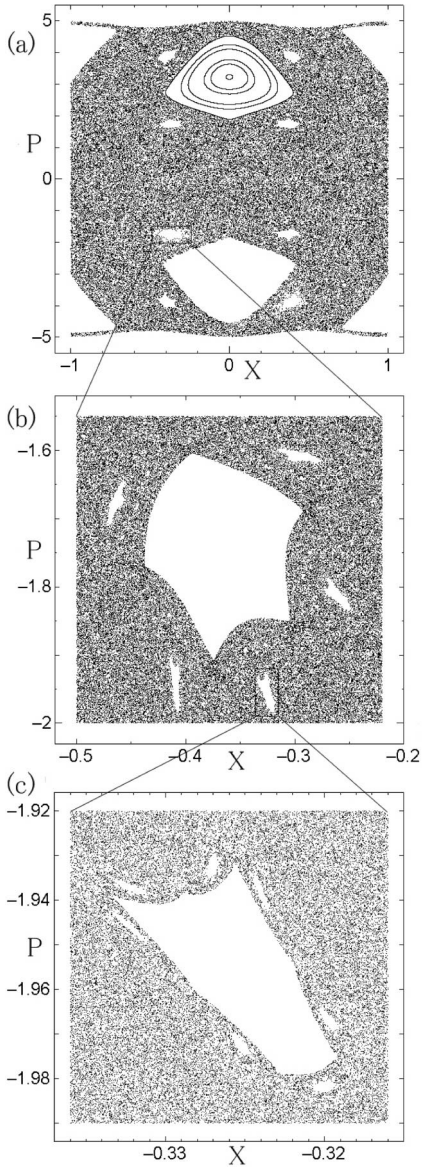

FIG. 5. (a) Poincaré section with $p=0$ at $E=6.21$. (b) Partial magnification of (a). (c) Partial magnification of (b).

First, we discuss the case $V_0=1$, where the AD appears clearly. A landscape of the two-dimensional potential is given in Fig. 2(a), and an example of phase dynamics is depicted in Fig. 2(b), showing both a smooth motion over barriers and a trapped motion in a potential valley. Our potential is periodic in the X direction but parabolic in the x direction. Thus the diffusive motion occurs in the X direction.[16] The time evolution of the center-of-mass for three initial conditions at $E=0.61$ is shown in Fig. 3(a). For this energy, three types of motion are observed, (i) drift, (ii) trapped-periodic, and (iii) diffusive motions, according to the initial conditions. The underlying Poincaré section with $p=0$ for $E=0.61$ is shown in Fig. 3(b), and is found to be composed of tori and chaotic sea. The central torus presents the trapped orbit, while the triplet of upper small tori corresponds to drift orbits. To investigate the diffusion phenomena, we hereafter focus on diffusive motions represented by

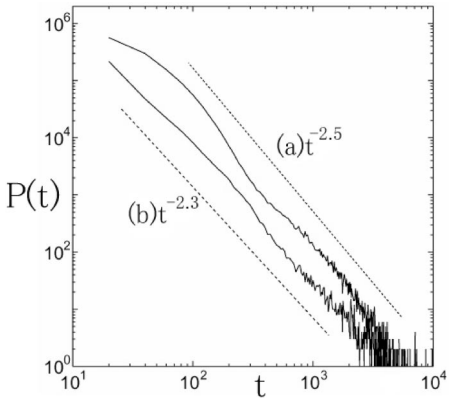

FIG. 6. (a) Jump-time distribution and (b) residence-time distribution at $E=1.26$.

the trajectories in the chaotic sea (iii). Therefore we have to choose the appropriate initial condition with constant total energy.

In order to quantify the diffusion property, we evaluate the mean square displacement (MSD) defined by

$$\sigma^2(t)=\langle[X(t)-X(0)]^2\rangle\sim t^{\alpha}, \tag{5}$$

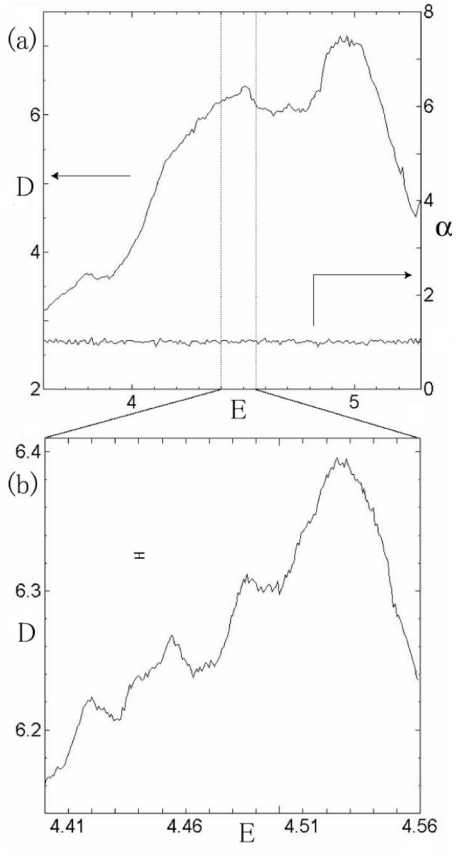

FIG. 7. Energy dependence of diffusion coefficient (a) for $3.6 \leqslant E \leqslant 5.3$ and (b) for the narrower region $4.40 \leqslant E \leqslant 4.56$. The exponent α is also shown in (a). The error bar in (b) is a typical statistical error of D.

where the exponent α characterizes the nature of diffusions. Figures 4(a), 4(b), 4(c), and 4(d) show MSD's which correspond to diffusions for $E=0.61$, 1.26, 3.01, and 6.21, respectively. The case $E=0.61$ shows normal diffusion ($\alpha=1$), while the latter three cases show the anomalous exponent $\alpha\sim1.5$. This enhanced diffusion is expected to be caused by a sequence of long-time jumps and long-time residences (trappings) as discussed below.[6,17,18]

To figure out details of AD, the corresponding Poincaré sections is shown in Fig. 5(a) for $E=6.21$. Figure 5(b) is a magnification of small island in Fig. 5(a) and Fig. 5(c) is a magnification of small island in Fig. 5(b) exhibiting the presence of a self-similar or hierarchy island structures. AD is expected to occur when an orbit enters into the hierarchy structure related to long-time jumps in the phase space.[2,10]

The property of AD is characterized by the jump-time and residence-time distributions. Figure 6 shows these distributions obtained numerically for $E=1.26$. The long-time tails obey approximately the power laws $P(t)\sim t^{-\gamma-1}$ and $\tilde{P}(t)\sim t^{-\tilde{\gamma}-1}$, for the jump-time and residence-time distributions, respectively. From Fig. 6 we find $\gamma\sim1.5$ and $\tilde{\gamma}\sim1.3$. According to the theory of the Lévy walk,[2,6] the exponent of the MSD is related to that of the jump-time and residence-time distributions as

$$\alpha=\begin{cases}2+\min\{\tilde{\gamma},1\}-\min\{2,\gamma\}, & \text{for} \quad \gamma>1,\\ 2+\min\{\tilde{\gamma},\gamma\}-\gamma, & \text{for} \quad 0<\gamma<1.\end{cases} \tag{6}$$

With use of the present convention ($\gamma=1.5,\tilde{\gamma}=1.3$), Eq. (6) yields $\alpha=1.5$ which is consistent with our observed value.

Next, we study the case $V_0=2$, which results in ND in a wide energy region. The normal diffusion in deterministic chaotic systems is not normal at all, and we show below that the diffusion constant has an irregular energy dependence. When the value of α in Eq. (5) is guaranteed to be unity, the diffusion coefficient can be determined as

$$D=\lim_{t\to\infty}\frac{1}{2t}\langle[X(t)-X(0)]^2\rangle. \tag{7}$$

Figure 7(a) shows the numerical results for the diffusion coefficient and the exponent α in the range $1.60<E<5.5$. In this energy domain, only ND with $\alpha=1$ occurs within the statistical error. Figure 7(b) is a magnification of a narrow region in Fig. 7(a), where the typical statistical error of D is also shown by an error bar. One can see clearly that D has a complicated fractal-like structure. This structure is numerically reproducible and is not due to statistical fluctuations in the numerical calculation. This amazing fractal-like feature is proper to the deterministic chaotic dynamics and is attributed to a sensitivity of the phase-space structure to the system's energy.[13]

Finally, we note that dynamics of SQUID's can be detected directly by an induced voltage V across the junction, which is related to the momentum of the center of mass through $V=P\hbar/2e\omega$. The correlation function of the center-of-mass momentum $C(t-t')=\langle P(t)P(t')\rangle$, can thus be obtained experimentally. The AD is characterized by the low-frequency part of the power spectrum $\tilde{C}(\omega)=\int dt\, e^{i\omega t}C(t)$ through $\tilde{C}(\omega)\sim\omega^{1-\alpha}$, while the ND is characterized by the diffusion constant $D\propto\tilde{C}(0)$.

In summary, we have studied the diffusion of superconducting phases in SQUID systems. Two kind of deterministic diffusions, anomalous diffusion (AD) and normal diffusion (ND) are investigated. For AD, the numerically-evaluated exponent of time in the mean square displacement is larger than 1, and is consistent with one derived by means of the jump-time and residence-time distributions. For ND, the diffusion coefficient D is shown to have a fractal-like feature as a function of the total energy. We hope future experiments on SQUID's to verify these novel features of deterministic diffusion predicted here.

We thank Dr. T. Harayama for a stimulating discussion on the irregular diffusion coefficients.

*Electronic address: tanimoto@a-phys.eng.osaka-cu.ac.jp

[1] P. Lévy, *Theorie de l'Addition des Variables Aleatoires* (Gauthier-Villiers, Paris, 1937).
[2] *Lévy Flights and Related Topics in Physics*, Lecture Notes in Physics Vol. 450, edited by M. F. Shlesinger *et al.* (Springer, Berlin, 1995).
[3] J. R. Dorfman, *An Introduction to Chaos in Nonequilibrium Statistical Mechanics* (Cambridge University Press, Cambridge, UK, 1999).
[4] J. Klafter *et al.*, Phys. Today **49**, 33 (1996).
[5] T. Geisel and S. Thomae, Phys. Rev. Lett. **52**, 1936 (1984).
[6] G. Zumofen and J. Klafter, Physica D **69**, 436 (1993).
[7] T. Geisel *et al.*, Phys. Rev. Lett. **54**, 616 (1985).
[8] R.F. Miracky *et al.*, Phys. Rev. A **31**, 2509 (1985).
[9] T.H. Solomon *et al.*, Phys. Rev. Lett. **71**, 3975 (1993).
[10] T. Geisel *et al.*, Phys. Rev. Lett. **59**, 2503 (1987).
[11] J. Klafter and G. Zumofen, Phys. Rev. E **49**, 4873 (1994).
[12] R. Klages and J.R. Dorfman, Phys. Rev. Lett. **74**, 387 (1995).
[13] T. Harayama and P. Gaspard, Phys. Rev. E **64**, 036215 (2001).
[14] A. Barone and G. Paterno, *Physics and Application of the Josephson Effect* (Wiley-Interscience, New York, 1982).
[15] Yu. Makhlin *et al.*, Rev. Mod. Phys. **73**, 357 (2001).
[16] Similar two-dimensional Hamiltonian systems whose potential is periodic in both directions are discussed in Refs. 10,11.
[17] M.F. Shlesinger *et al.*, Phys. Rev. Lett. **58**, 1100 (1987).
[18] A. Blumen *et al.*, Phys. Rev. A **40**, 3964 (1989).